

# Electric Power Steering System Design Based on Linear Quadratic Control

Tomokazu Abe<sup>1,a</sup>, Yu Fujimura<sup>1</sup>, Tatsuya Hirose<sup>1</sup>, Seiji Hashimoto<sup>1,b</sup>,  
Mitsunobu Kajitani<sup>2,c</sup>, Ken Sato<sup>3</sup>, and Kazuhiko Gonpei<sup>3</sup>

<sup>1</sup> Gunma University, 1-5-1 Tenjin, Kiryu, Gunma, 376-8515, JAPAN

<sup>2</sup> Aichi University of Technology, 50-2 Nishihassama, Gamagori, Aichi, 443-0047, JAPAN

<sup>3</sup> Diamond Electric Mfg. Co. Ltd., 1-15-27 Tsukamoto, Yodogawa-ku, Osaka, 532-0026 JAPAN

<sup>a</sup><TOMOKAZU\_ABE@po.diaelec.co.jp>, <sup>b</sup><hashimotos@gunma-u.ac.jp>, <sup>c</sup><kajitani@aut.ac.jp>

**Keywords:** EPS, linear quadratic, disturbance observer, disturbance rejection

**Abstract.** Electric power steering (EPS) systems are gradually replacing hydraulic power steering in modern cars. The main advantages of the EPS systems are their lower energy consumption and potential applications in autonomous driving.

This paper discusses linear quadratic (LQ) control to reduce effort- and time-consuming manual tuning and to improve the steering feel compared to conventional map control. Moreover, a disturbance observer is introduced to estimate and suppress disturbances due to mechanical resonance and the self-aligning torque. The effectiveness of different combinations of these controllers is evaluated with simulations and hardware-in-the-loop (HIL) simulator-based experiments.

## 1. Introduction

Among the actuators of modern cars, the steering system is the one that most influences the vehicle's maneuverability [1]. Electric power steering (EPS) systems complement manual steering with an electric motor, and are gradually replacing conventional hydraulic power steering systems in modern cars because of their fuel efficiency and potential applications in autonomous driving [2]. For these reasons, the EPS market is expanding rapidly [3].

To steer an automobile electronically, the steering torque, steering angle, and vehicle speed are transmitted to the engine control unit. These signals are used to calculate the best assisting torque for the driver from the assist boost curve and compensation map. Fig. 1 shows the control structure of an EPS system. Compensation maps are based on a combination of the viscosity compensation, inertia compensation and so on [4],[5]. To improve the steering feel, methods using these compensators have been extensively reported on in the literature [6],[7]. However, these methods are often very complicated, because they depend not only on the steering torque, vehicle speed, and steering angle but also on many other nonlinear factors [8]. Consequently, far fewer studies have considered the consolidation and simplification of compensation. In practice, the EPS control systems are designed through trial and error, which means that the performance of the systems depends on the skill of experts, and their development is a time-consuming task [9].

This paper deals with the potential of linear quadratic (LQ) control to reduce the time and effort required for manual tuning in EPS systems, and to improve the steering feel compared to the conventional compensation map control. Moreover, a disturbance observer is introduced to estimate and suppress disturbances from the mechanical resonance and self-aligning torque.

In Sections 2 and 3, a disturbance observer-based LQ control system that is labor-saving and more robust to disturbances is presented. Moreover, the effectiveness of the proposed method is compared with the conventional method in simulations and hardware-in-the-loop (HIL) simulator-based experiments in Section 4. Finally, our findings are summarized in Section 5.

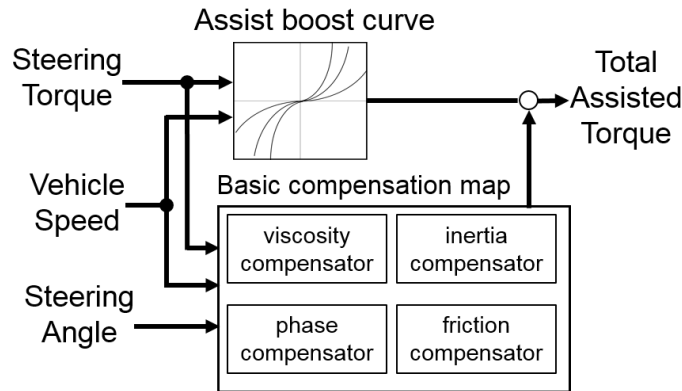


Fig. 1. Control structure of the EPS system.

## 2. Linear Quadratic Control Method Compensated with Disturbance Observer

### 2.1 Modeling of EPS

This section introduces the mathematical model for the EPS system. Fig. 2 shows an illustration of the physical components of an EPS system. The EPS system can be expressed with the following equations of motion

$$\begin{cases} I_h \ddot{\theta}_h + K_h(\theta_h - N_t \theta_T) = T_h & (1) \end{cases}$$

$$\begin{cases} I_m \ddot{\theta}_m + \frac{K_h(N_t \theta_T - \theta_h)}{N_m} + N_m N_t T_T = T_m & (2) \end{cases}$$

$$\begin{cases} I_T \ddot{\theta}_T + C_T \dot{\theta}_T + K_T \theta_T = T_T & (3) \end{cases}$$

where subscripts  $h$ ,  $m$ , and  $T$  represent the steering wheel, the assist motor, and the tire, respectively. Here,  $I$ ,  $\theta$ , and  $T$  denote the inertia, angle, and torque, respectively.  $K_h$  and  $K_T$  are the spring constant of the torsion bar and tire, respectively.  $N_t$  and  $N_m$  are the reduction ratio of the steering wheel and the assist motor, respectively.  $C_T$  represents a damper coefficient for the tire.

In (1)–(3), the reduction ratios differ among the steering shaft, assist motor, and tire, and are measured along the tire axis. The uppercase subscript indicates values transformed to the tire axis. Applying these conversions, the following equations are obtained.

$$\begin{cases} I_H \ddot{\theta}_H + K_H(\theta_H - \theta_M) = T_H & (4) \end{cases}$$

$$\begin{cases} I_M \ddot{\theta}_M + C_T \dot{\theta}_M + K_H(\theta_M - \theta_H) = T_M & (5) \end{cases}$$

where  $\theta_T = \theta_M$  and  $I_M = (N_t N_m)^2 I_m + I_T$ .

For the state variables  $[\theta_H \quad \dot{\theta}_H \quad \theta_M \quad \dot{\theta}_M]^T$ , the state space model is given by

$$\begin{pmatrix} \dot{\theta}_H \\ \ddot{\theta}_H \\ \dot{\theta}_M \\ \ddot{\theta}_M \end{pmatrix} = \begin{pmatrix} 0 & 1 & 0 & 0 \\ -\frac{K_H}{I_H} & 0 & \frac{K_H}{I_H} & 0 \\ 0 & 0 & 0 & 1 \\ \frac{K_H}{I_M} & 0 & -\frac{K_H+K_T}{I_M} & -\frac{C_T}{I_M} \end{pmatrix} \begin{pmatrix} \theta_H \\ \dot{\theta}_H \\ \theta_M \\ \dot{\theta}_M \end{pmatrix} + \begin{pmatrix} 0 \\ 0 \\ 0 \\ \frac{1}{I_M} \end{pmatrix} T_M + \begin{pmatrix} 0 \\ \frac{1}{I_H} \\ 0 \\ 0 \end{pmatrix} T_H \quad (6)$$

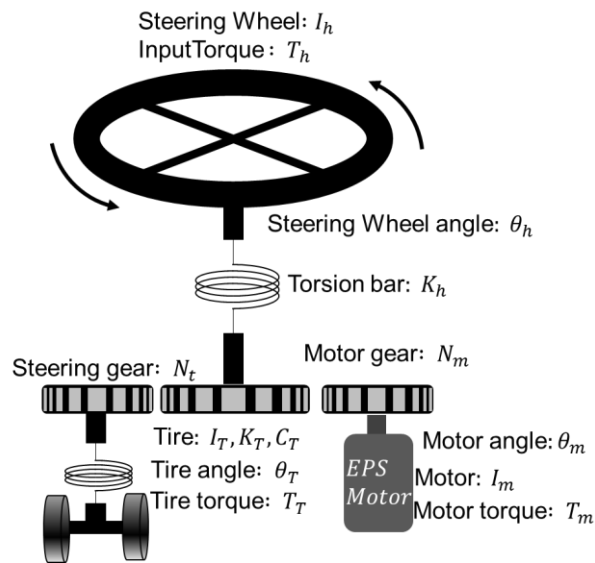


Fig. 2. Basic Components of the EPS system.

## 2.2 Torsional torque-based assist control system design

The assist motor reduces the manual steering torque. Here,  $K_{as}$  denotes the assist torque gain. Then, the basic motor torque,  $T_M$ , can be expressed by

$$T_M = K_{as}K_H(\theta_H - \theta_M). \quad (7)$$

## 2.3 Torsional torque-based assist control system design with disturbance observer

To compensate for the self-aligning torque and other low-frequency disturbances due to the mechanical resonance, the disturbance observer expressed by (8) is applied to the motor torque  $T_M$ . Here,  $P_n(s)$  represents the nominal model of the EPS system, and  $F(s)$  is a low-pass filter for converting  $P_n^{-1}(s)F(s)$  to the proper transfer function. A block diagram of the system is shown in Fig. 3.

$$T_M = K_{as}K_H(\theta_H - \theta_M) + P_n^{-1}(s)F(s)(P_n(s)T_M - \theta_H) \quad (8)$$

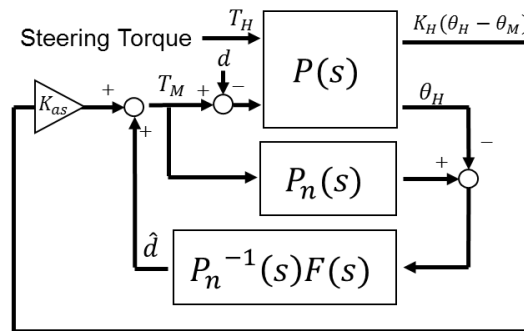


Fig. 3. Block diagram of the assist control method with disturbance observer.

### 2.4 Simulation results

In this section, the effectiveness of the disturbance observer is evaluated by comparing the control systems expressed by (7) and (8). The response of  $\theta_H$  and the motor torque when applying the step signal to the steering torque  $T_H$  at  $t = 1.0$  s are shown in Figs. 4 and 5. Noted that a sine wave of 7 Hz is added to  $T_M$  as a low-frequency disturbance  $d$  at  $t = 6.0$  s. Here, DO represents the disturbance observer. Fig. 6 shows the behavior of the input disturbance and the disturbance estimated by the system. The DO estimation is able to reproduce the amplitude and phase of the input disturbance. A comparison of the steering angles,  $\theta_H$ , with and without DO, is shown in Fig. 7. From these results, it is confirmed that the DO-based control system reduces the vibrations resulting from the sinusoidal disturbance. The vibration amplitude ratio of the proposed method to the conventional one is 50.0%.

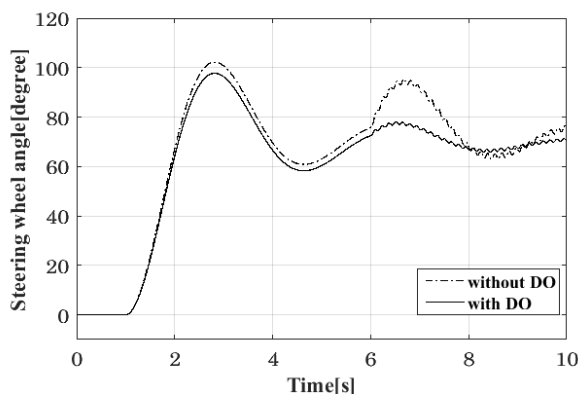


Fig. 4. Comparison of step responses  $\theta_H$  with and without the disturbance observer.

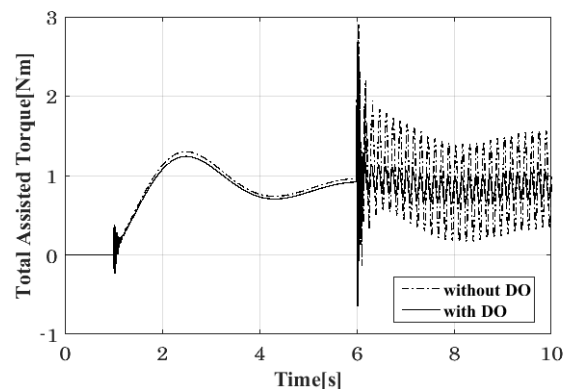


Fig. 5. Comparison of step responses  $T_M$  with and without the disturbance observer.

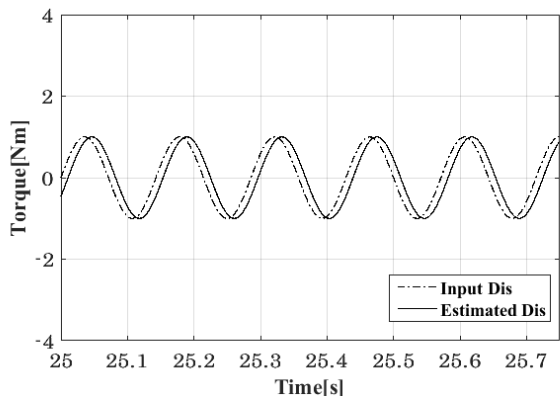


Fig. 6. Comparison of the input disturbance and the estimated disturbance.

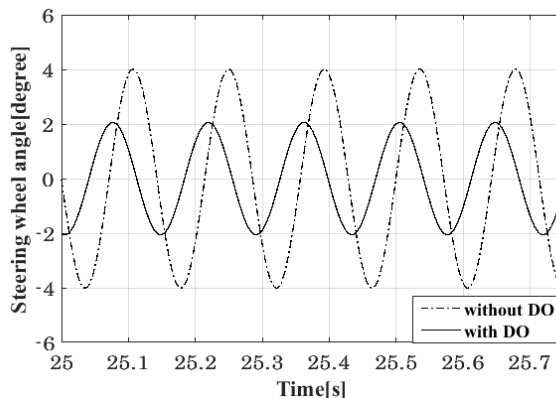


Fig. 7. Comparison of sinusoidal responses  $\theta_H$  with and without the disturbance observer.

### 2.5 Assist control system with viscosity compensation

In addition to the EPS system expressed by (7), it is necessary to ensure that the assisted steering is stable and suitable for human response times by adding a damping force. To meet these requirements, the motor control torque  $T_M$  is applied with viscosity compensation as in (9), which is one of the conventional methods. In (9),  $K_{CT}$  represents the viscosity compensation gain.

$$T_M = K_{as}K_H(\theta_H - \theta_M) - K_{CT}C_T\dot{\theta}_M \tag{9}$$

### 2.6 Assist control system design with a disturbance observer and linear quadratic control

In the proposed method, the motor control torque  $T_M$  based on the LQ control with a disturbance observer, as described in (10), is introduced instead of the viscosity compensation.

$$T_M = K_{as}K_H(\theta_H - \theta_M) + P_n^{-1}(s)F(s)(P_n(s)T_M - \theta_H) - F_{LQ}\theta \tag{10}$$

Here,  $\theta = [\theta_H \ \dot{\theta}_H \ \theta_M \ \dot{\theta}_M]^T$ , and  $F_{LQ}$  represents the state feedback gain of the LQ control. The block diagram is shown in Fig. 8.

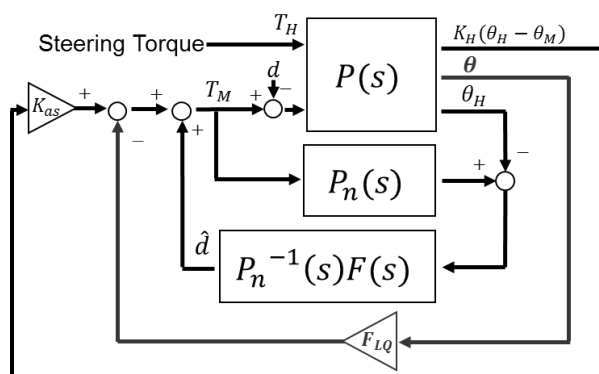


Fig. 8. Block diagram of LQ control method with disturbance observer.

### 2.7 Simulation results

In this section, the robustness of the low-frequency disturbances in the assist control method expressed by (9) and the control method by (10) are compared in simulations. The responses of  $\theta_H$  and the motor torque when applying the step signal to the steering torque  $T_H$  at  $t = 1.0$  s are shown in Figs. 4 and 5. Noted that a sine wave of 7 Hz is added to  $T_M$  as a low-frequency disturbance  $d$  at  $t = 6.0$  s. The proposed method can better suppress the vibration and the transient vibrations than the conventional method with respect to the sinusoidal disturbance. The vibration amplitude ratio of the proposed to the conventional method is 50.0%. Therefore, the proposed method shows the same improvement in performance as the method with the disturbance observer, and it can therefore replace the conventional method.

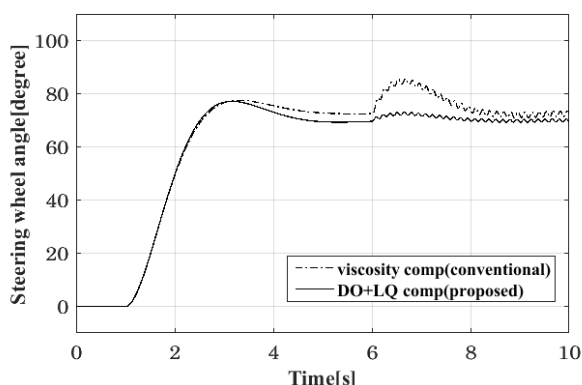


Fig. 9. Comparison of step responses  $\theta_H$  by the conventional and proposed methods.

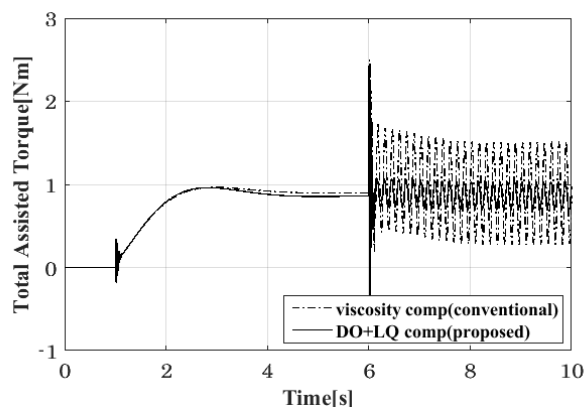


Fig. 10. Comparison of step responses  $T_M$  by the conventional and proposed methods.

## 3. Linear Quadratic Control Method with Disturbance Observer and State Estimation Observer

### 3.1 Full-order state observer design

The state feedback control is theoretically straightforward; however, its application in practical situations is complex. In Section 2, it was assumed that all state variables are observable. Nevertheless, state variables cannot always be directly measured by the physical sensors in the EPS system. To measure the state feedback, the state observer shown in (11) is introduced. The combined block diagram is shown in Fig. 11. The state equation of the observer for the EPS system expressed by (11) is given as

$$\dot{\theta} = A\hat{\theta} + Bu + L(C\hat{\theta} - y) \quad y = C\hat{\theta} \quad (11)$$

$$A = \begin{pmatrix} 0 & 1 & 0 & 0 \\ -\frac{K_H}{I_H} & 0 & \frac{K_H}{I_H} & 0 \\ 0 & 0 & 0 & 1 \\ \frac{K_H}{I_M} & 0 & -\frac{K_H + K_T}{I_M} & -\frac{C_T}{I_M} \end{pmatrix}, \quad B = \begin{pmatrix} 0 \\ 0 \\ 0 \\ \frac{1}{I_M} \end{pmatrix}, \quad C = (1 \quad 0 \quad 0 \quad 0)$$

The motor control torque,  $T_M$ , based on the LQ control with a disturbance observer and state estimation observer is described in (12). Here,  $\hat{\theta}$  is introduced instead of  $\theta$ .

$$T_M = K_{as}K_H(\theta_H - \theta_M) + P_n^{-1}(s)F(s)(P_n(s)T_M - \theta_H) - F_{LQ}\hat{\theta} \tag{12}$$

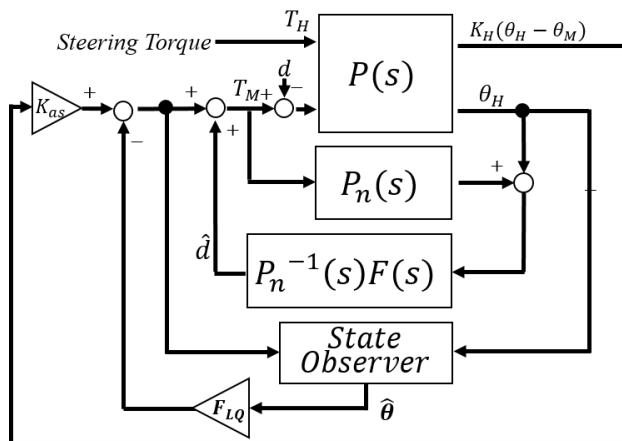


Fig. 11. Block diagram of LQ control method with disturbance observer and state estimation observer.

### 3.2 Simulation results

In this section, simulations are conducted to clarify the robustness of the low-frequency disturbance in the assist control method expressed by (9) and the control method by (12). The time response of  $\theta_H$  and the motor torque when applying the step signal to the steering torque  $T_H$  at  $t = 1.0$  s are described in Figs. 12 and 13. The simulation conditions are the same as in Section 2.7. In Fig. 12, SO denotes the state estimation observer. The effect of the low-frequency disturbance is also smaller than for the conventional method. The performance of the proposed method with the state estimation observer is approximately equal to the one without the state estimation observer. From the results, it is noted that the proposed method is valid even if some of the state variables are not observable.

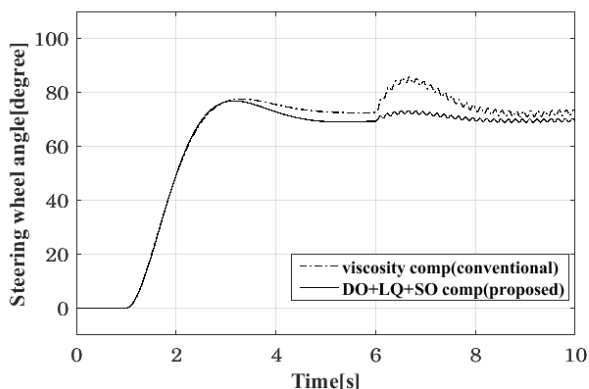


Fig. 12. Comparison of step responses  $\theta_H$  by the conventional and proposed methods with the state estimation observer.

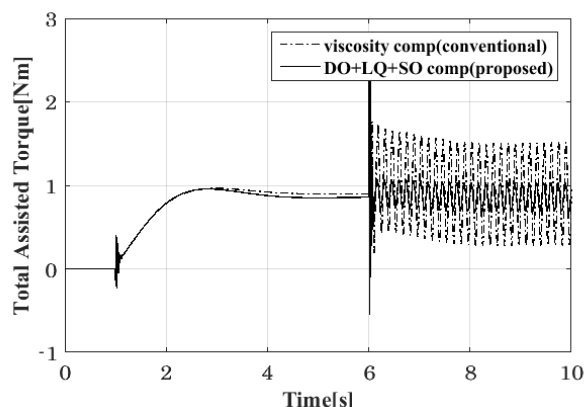


Fig. 13. Comparison of step responses  $T_M$  by the conventional and proposed methods with the state estimation observer.

#### 4. Hardware-In-The-Loop Experiment

Simulations under a variety of settings were performed to evaluate the proposed EPS control system as mentioned in the previous section. To verify the proposed control method effectively, a HIL system was constructed. In the HIL experiment, the load motor was attached to a rack-and-pinion gear to generate various load torques which are delivered from the road to the steering shaft. Figs. 14 and 15 show the structure of the HIL system.

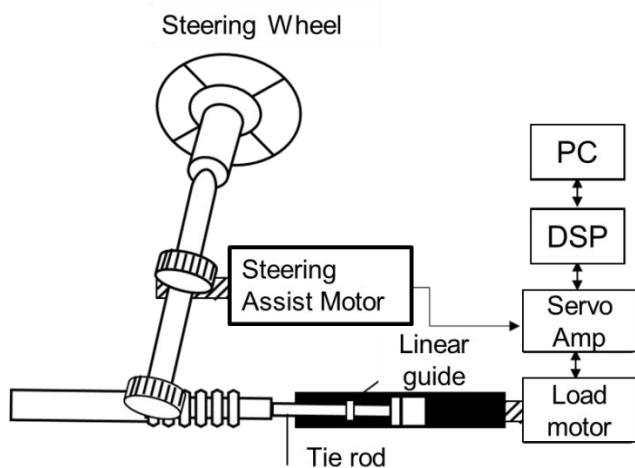


Fig. 14. Structure of the HIL system.

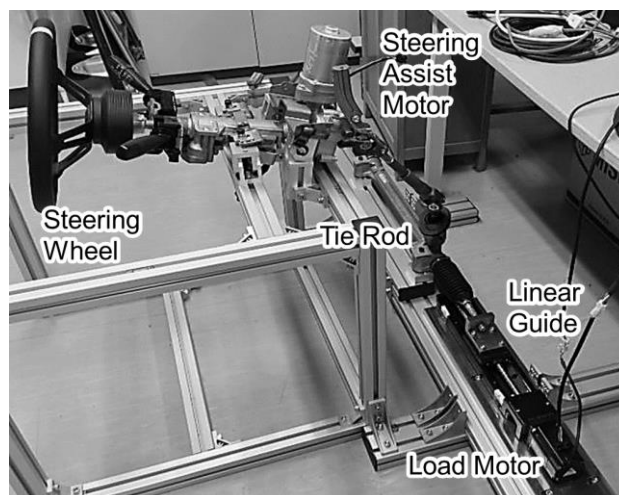


Fig. 15. HIL system.

The results for the disturbance estimation experiment with the disturbance observer are shown in Fig. 16, where the assist torque reference and the load torque reference are produced by DSP using  $\theta_H$ . It is noted that a sine wave of 7 Hz is added to  $T_M$  as a low-frequency disturbance,  $d$ . Despite the lag and noise, the disturbance observer has the ability to accurately estimate the sinusoidal disturbance.

Fig. 17 shows the response of  $\theta_H$  when applying a sine wave of 7 Hz as a low-frequency disturbance to the motor torque  $T_M$ . The vibration amplitude ratio of the control method with the disturbance observer to the control method without one is 66.2%. It is noted that the control system for the DO-based proposed method expressed by (10) is suitable for suppressing vibrations.

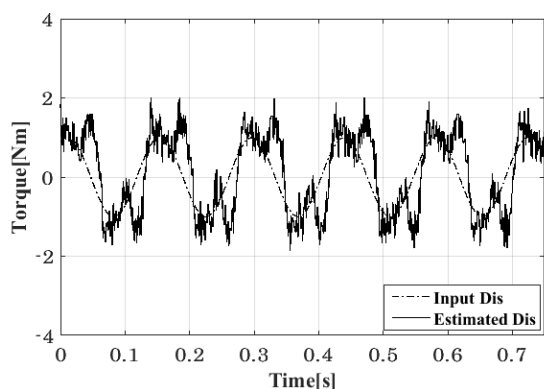


Fig. 16. Comparison of input disturbance and estimated disturbance in the HIL-based experiment.

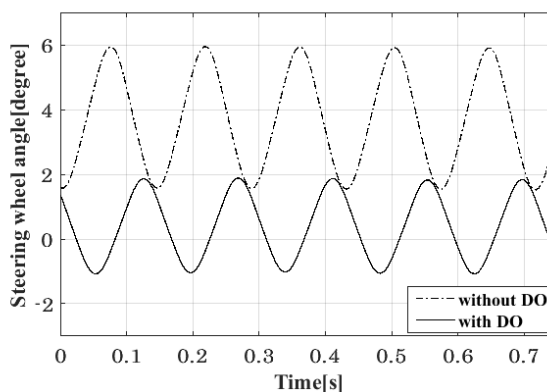


Fig. 17. Comparison of sinusoidal responses  $\theta_H$  with and without disturbance observer in the HIL-based experiment.

The response of  $\theta_H$  when applying the step signal to the motor torque  $T_M$ , which is equivalent to the steering assist torque at  $t = 18.0$  s, is shown in Fig. 18. It is noted that a sine wave of 7 Hz is also added to  $T_M$  as a low-frequency disturbance at  $t = 23.0$  s. The experimental results indicate that the proposed method can reduce the vibrations and improve the transient response to the disturbances. The rise time of the proposed method is also shorter than that of the conventional method. It can be concluded that the proposed method is more robust to disturbances than the conventional method.

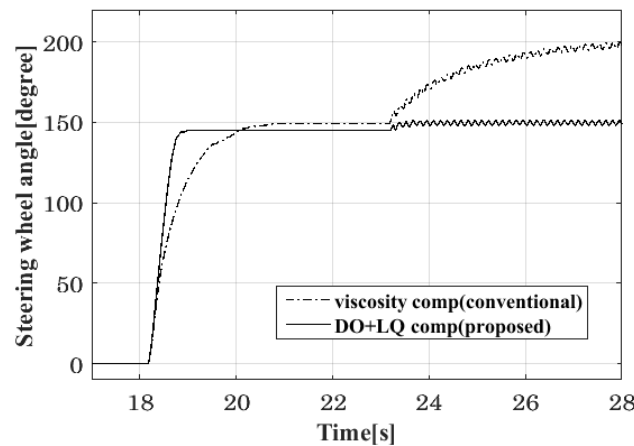


Fig. 18. Comparison of the step responses  $\theta_H$  for the conventional and proposed method in the HIL-based experiment.

## 5. Conclusion

This paper has discussed a linear quadratic (LQ) based EPS control system to reduce the need for effort- and time-consuming manual tuning and to improve the steering feel compared to conventional map control. A disturbance observer was introduced to estimate and suppress disturbances from the mechanical resonance and self-aligning torque. The effectiveness of different combinations of these controllers was evaluated with simulations and HIL experiments. Future work will include a comparison of the proposed control method and the conventional map compensation in the HIL system.

## References

- [1] S.Fankem, T.Weiskircher, S.Mller, "Model-based Rack Force Estimation for Electric Power Steering", *19th IFAC World Congress*, Vol.47, Issue 3, pp.8469-8474, 2014.
- [2] K.Kondo and H.Kubota, "Innovative Application Technologies of AC Motor Drive Systems.", *IEEJ Journal of Industry Applications*, Vol.1, No.3, pp.132-140, 2012.
- [3] Mathias Wurges, "New Electrical Power Steering Systems", *IEEJ Transactions on Electrical and Electronic Engineering Online*, 2013.
- [4] M.K.Hassan, N.A.M.Azubir, H.M.I.Nizam, S.F.Toha, B.S.K.K.Ibrahim, "Optimal Design of Electric Power Assisted Steering System (EPAS) Using GA-PID Method", *International Symposium on Robotics and Intelligent Sensors 2012*, Vol.41, pp.614-621, 2012.
- [5] D.Watanabe, M.Kataoka, T.Fujii, M.Iwase, "Development of Electric Power Steering Control based on Alignment Torque", *Denso Technical Review*, Vol.15, pp.69-71, 2010.

- [6] S.Takehara and T.Yoshioka, "Improvement of Steering and Vehicle Characteristics due to Electric Power Assist Steering with Disturbance Observe.", *Transactions of the JSME* , Vol.70, No.835, 2004.
- [7] J.Kim and J.Song, "Control logic for an electric power steering system using assist motor.", *Mechatronics* , Vol. 12, Issue 3, pp. 447459, 2002.
- [8] B.Yi, J.Ferdinand, N.Simm, F.Bonarens, "Application of Local Linear Steering Models with Model Predictive Control for Collision Avoidance Maneuvers", *IFAC-PapersOnLine*, Vol.49, Issue 15, pp.187192, 2016.
- [9] Y.Saitho, H.Itoh, F.Ozaki, T.Nakamura, S.Kawaji, "Design Method for EPS Control System Based on KANSEI Structure", *IEEJ Transactions on Industry Applications*, Vol.130, No2, 2010.
- [10] E.Saito and S.Katsura, "Position Control of Resonant System with Load Force Suppression Using Wave Observer", *IEEJ Journal of Industry Applications*, Vol.3, No.1, pp.18-25, 2013.
- [11] T.Hiraide, K.Takahashi, M.Nandavapa and K.Ohishi, "Fine Acceleration Control Method Considering Torque Ripple for Hybrid-Type Stepping Motor", *IEEJ Journal of Industry Applications*, Vol.3, No.1, pp.18-25, 2013.
- [12] D.Wang, C.Li, D.Liu, C.Mu, "Data-based robust optimal control of continuous-time affine nonlinear systems with matched uncertainties", *Information Science*, Vol.366, pp. 121-133, 2016.
- [13] J.Lu, P.Wang b, Z.Zhan, "Active vibration control of thin-plate structures with partial SCLD treatment", *Journal of Mechanical Systems and Signal Processing*, Vol.84, Part A, pp.531-550, 2016.
- [14] V.Piccirillo, J.M.Balthazar, A.M.Tusset, D.Bernardini, G.Regia, "Application of a Shape Memory Absorber in Vibration Suppression", *Applied Mechanics and Materials*, Vol. 849, pp. 27-35, 2016
- [15] V.Yanchevskiy, E.Yanchevskaya, "Mathematical Model of Tire Life Calculation in Real Conditions", *Applied Mechanics and Materials*, Vol.838, pp. 78-84, 2016